

EMPIRICAL Z-VISIBILITY RELATION FOUND BY FOG MEASUREMENTS AT AN AIRPORT BY CLOUD RADAR AND OPTICAL FOG SENSORS

Matthias Bauer-Pfundstein^{*}
Gerhard Peters
Bernd Fischer
METEK GmbH, Elmshorn, Germany

1. INTRODUCTION

A scanning K-band cloud radar (MIRA-36) was operated at the airport Munich during the winter 2011/2012 for observing fog. The measurements took place in the frame of the iPort project (innovative airport) funded by German government for improving safety and efficiency of air traffic. For detecting fog, where it is most interesting for the air traffic management, the radar was tilted towards the gliding path at an elevation of 5°. The radar was set to a range resolution of 30 m and the minimum range is 150 m. Therefore a height resolution of 2.6 m beginning at 16 m above ground is obtained. In a 15 min cycle also azimuth scans at 45° elevation were performed to get information about the cloud coverage above the airport, which is important for the fog prediction.



Fig. 1 Scanning MIRA-36 mounted on a trailer at the Munich airport with antenna pointing towards the gliding path (elevation=5°)

In contrast to optical methods the radar provides range resolved information far beyond the range of optical visibility. On the other hand it is not a priori obvious, if there is significant correlation between the radar reflectivity and visibility. Due to the D^6 -dependence of the radar reflectivity factor Z and the D^2 -dependence of the visibility length (D = drop size diameter) the Z-Visibility relation depends on the drop size distribution. One goal of the field campaign was to determine a first estimate of a Z-Vis relation by making scatter plots (or two-dimensional histograms) of the reflectivity factors

measured by the cloud radar versus the visibility measurements from optical instruments. From such Z-Vis scatter plots the minimal radar sensitivity required to detect all fog events that are critical for air traffic management can be deduced. Also the accuracy of Z-Vis relations can be estimated from this empirical data.

The visibility values needed for this investigation were taken from the following sources:

- Runway visual range transmissometers (RVR). These Instruments are installed at a height of 2 m above the runway. The lowest Range gate of the cloud radar during most time of the field campaign was at 16 m. As fog density typically changes quite much between these two altitudes the correlation between the radar reflectivities RVR visibilities was not very good.
- During the field campaign a Jenoptic CHM15kx ceilometer was located 400 m to the east of the radar. As during gliding path measurements the radar beam was tilted to the direction of the ceilometer the radar beam intersected the Ceilometer beam at a height of 35 m. A method was developed to estimate the extinction of the ceilometer signal by using the height profiles of the signal intensities of the radar and the ceilometer (see Section 5).
- METAR Visibility: The visibility estimated by human weather observers represents an average over the height where the observer is located (~50 m above ground in the airport tower) and targets at the ground used by the observers for estimating the visibility length. The METAR visibilities correlate best with the radar reflectivities between 25 and 35 m height.

In the sections 3 to 5 these different visibility measurements will be exploited for gaining a Z-Vis relation. The following section gives some details about how the cloud radar was used for detecting fog.

2. MEASURING FOG BY A CLOUD RADAR

The operational parameters of the radar used during the field campaign are listed in the Table 1.

Radar frequency	35.45 GHz
Pulse Power	30 kW
Average Power	30 W
Antenna diameter /gain/beam width	1 m / 49.7 dBi / 0.5°

^{*} Corresponding author address: Matthias Bauer-Pfundstein, METEK GmbH, Fritz-Strassmann Str. 4, 25337 Elmshorn, Germany +494121 4359 22, bauer@metek.de

Transmitting Pulse Length / Pulse Repetition Frequency	200 ns / 5000 Hz corresponding to 30 m range gates / ± 10 m/s velocity ambiguity range
Polarization	Horizontally on transmit and two receivers for Co- and Cross polarized signal
Number of pulses used per FFT	256 corresponding to a velocity resolution of 8 cm/s
Incoherent averaging	100 power spectra corresponding to 5 s time resolution
Minimal sensitivity at 1 km range (Z_1)	-65 dBZ (with the parameters given above and averaging)

Table. 1 Specifications and operational parameters of the cloud radar used during the field campaign.

The minimum measuring range of the radar is 150 m. To be able to observe fog at lower heights (above ground) the radar beam was tilted to lower elevations than normally used for cloud observation. An elevation of 5° with respect to horizon was chosen. Like this the first range gate (150 m) is at a height of $\sin(5^\circ) \cdot 150 \text{ m} + \text{height of radar antenna} = 13 \text{ m} + 2.8 \text{ m} = 16 \text{ m}$. Lower elevations down to 3° were tested to achieve lower minimum heights and finer height resolutions and to measure the fog exactly on the gliding path of landing aircrafts. But on the other hand at lower elevations fog at a given height appears at greater ranges and therefore the sensitivity suffers from tilting the beam too low. As before the field campaign it was not clear in which dBZ range the reflectivity of fog will be the settings where chosen to allow detecting very small dBZ values. For this reason during the first 2.5 months of the field campaign the elevation was set to 5° and also no scanning was done during 7 minutes of each quarter hour which allows extending the spectra averaging if more sensitivity would have been needed. After looking at the dBZ values of about 20 fog events during the first 2.5 months of the field campaign we concluded that a sensitivity of $Z_1 = -60$ to or even -55 dBZ should be sufficient. So we reduced spectral averaging to 1 s and started RHI-scanning. See section 6.

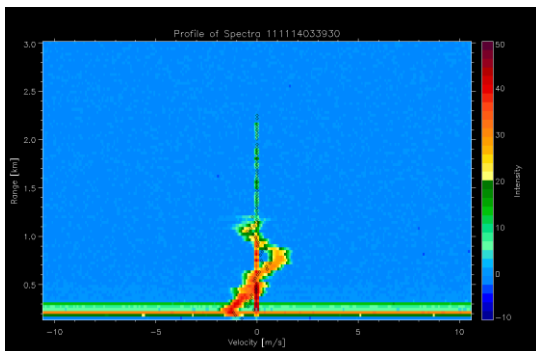


Fig. 2 Doppler spectra in the range gates from 150 m to 3000 m. Ground clutter can be seen at velocities close to 0 m/s. The signal from fog has wider peaks.

When pointing the beam to low elevations the ground clutter due to side lobes increases. In the beginning of the experiment we tested carefully how low the beam can be tilted without saturating the receiver by ground clutter. Fortunately the ground clutter was less intense than expected. Figure 2 shows a range profile of spectra recorded at an elevation of 3° above horizon. We did not steer the beam to elevations below 3° because we did not want to hit buildings or the tower by the radar beam.

Even during scanning the ground clutter has a small spectral width, which is mainly determined by the FFT window. Therefore it can be identified in the spectra quite easily.

Due to the low elevation sometimes a tremendous amount of signal from plankton (insects or other flying objects) is in the data. It can be distinguished from fog by its linear de-polarization ratio (LDR), the ratio between the receiving signal with 90° rotated polarization of the electromagnetic field and the receiving signal scattered with the same polarization as the transmitted signal. Fog consists of spherical droplets (even below melting temperature). Therefore the radar waves scattered at fog have the same polarization as the transmitted signal. The signal from plankton typically has LDR values -15 dB or more. For distinguishing between fog and plankton an LDR threshold of -17 dB has been used. Fortunately during fog events there is not much plankton in the data. Also plankton targets typically have high enough signal power so that even the cross channel power is high enough so that they can clearly be identified. The software is able to identify several peaks in the Doppler spectrum of each range gate. Each peak is classified separately. Therefore the plankton removal does not remove too many peaks from fog.

Aircrafts have been seen rarely in the radar signal during the field campaign though the radar was pointed only about 1.5° above the gliding path. If an aircraft hits the radar beam or a side lobe the plankton removal algorithm discards the signals.

During most of the time of the field campaign (11.11.2011 to 21.2.2012) the following scanning procedure was performed periodically every 15 minutes. At the beginning the beam is pointing towards the gliding path at an elevation of 5° and an azimuth of 82° (see Fig. 5). Then the following scanning was performed:

- RHI scan from 5° to 45° elevation during 100 s.
- Full circle PPI at elevation 45° during 300 s.
- RHI scan from 45° to 5° elevation during 100 s.
- The beam remains at 5° elevation and azimuth= 82° (gliding path) for the remaining 400 s of the quarter hour

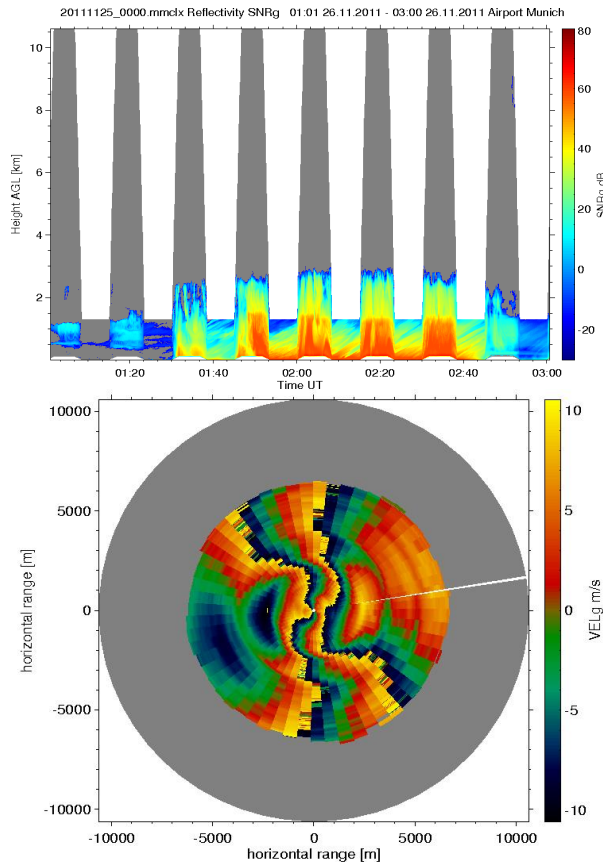


Fig. 3 Upper picture: Signal to noise ratios of the radar co-channel showing 2 hours of the scanning procedure during rain. On the y-axis the height = range * $\sin(\text{elevation})$ is plotted. Therefore during the gliding path measurements data is available in the height range from 16 m to 1.3 km and during the PPI scan from 110 m to 10.6 km. The height-time-ranges where no data is available are plotted in white. The height-time-ranges where the radar signal is below the noise threshold are plotted grey. **Lower picture:** VAD (velocity azimuth display) of one of the quarter hourly PPI scans (300 s, elevation=45°, azimuth=1.2°/s)

The last 400 seconds of each cycle are most useful for fog measurements as the elevation setting of 5° allows measuring down to 16 m above ground. The PPI scan was made to get information about the cloud coverage, which may help to make a short term prediction of fog. From the PPI scan it is also possible to deduce the direction and speed of the horizontal wind by using a VAD algorithm. After velocities are unfolded by the VAD algorithm also a rough estimate of the falling velocities can be deduced from the PPI scan. For deciding whether the radar signal is caused by fog or drizzle it is very useful to determine the falling velocity. From the PPI scan the falling velocity can be determined from a bit lower height than from vertically pointing measurements. To get information about the droplet falling velocities at even lower altitudes the data from RHI scans can be used (see section 6).

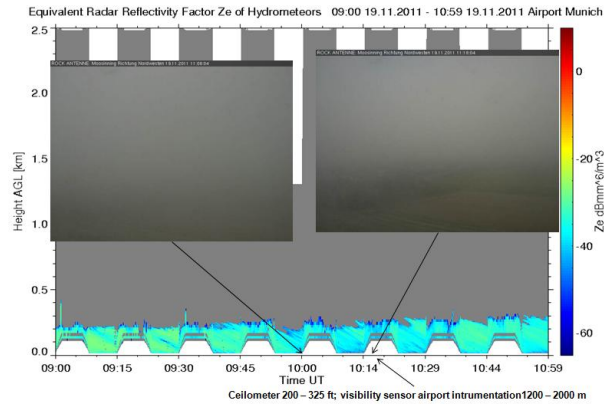


Fig. 4 Radar Reflectivity Factor (dBZ) during a fog event together with photos from a nearby webcam.

In Fig. 4 an example is shown where strong fog, which had developed during night, lifted few meters off the ground. Therefore the visibility sensors indicated rather high visibilities between 1200 m and 2000 m (2000 m is the highest visibility indicated by these sensors). The ceilometers of the airport instrumentation indicate a "ceiling height" of about 200 m. The radar data indicate that there is a rather homogeneous fog layer with a top height of 210 to 290 m. It is deep enough so that it can also be seen during the periods with 45° Elevation but in the 1st and 3rd range gate the sensitivity of the radar is not good enough to detect the fog. At 10:10 UTC it can be seen that the fog had lifted a bit. The webcam photo shows that the fog is still quite significant.

3. EMPIRICAL Z-VIS RELATION FROM RVR AND METAR VISIBILITIES

In the period from Nov. 11th to Feb. 21st at 17 days fog was encountered. The data of all these days (17 X 24 h, not only during the fog periods) was used for investigating the Z-Vis relation. After ground clutter and plankton filtering the reflectivity values of the 7 minutes of each quarter hour, during which the beam was dwelled at 5° elevation, were averaged to get one height profile of Z values. This averaging of Z does not increase the sensitivity, because values < Z_1 were discarded. It was mainly done because the RVR and METAR visibility data was not exactly from the same place as the radar measurements and specially the visibility length from human observers was available only twice per hour. The correlation of these shifted observations was improved by averaging.

To eliminate the periods with rain a simple algorithm was used. A fog layer that is thinner than the minimum range of the radar (150 m) normally does not produce rain. For this reason rain can be detected by pointing the radar vertically. In this case it can be deduced from the falling velocities if it is raining. Unfortunately the beam was not directed vertically during the whole period. Instead we assumed the signal to be rain if the signal layer height was higher than 500 m. The height of the signal layer was defined as the height where the dBZ values falls 10 dB below the average of the profile

below. If the signal layer height was above 500 m the signal was declared as rain. For similar measurements in future the droplet falling velocities should be measured either by making measurements with vertical beam or by RHI scans.

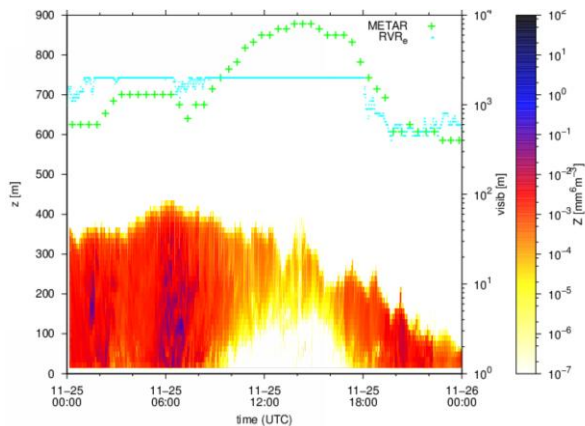


Fig. 5 Time-height cross section of the radar reflectivity Z and time series of the visibility length (scale on the right side) measured by the RVR_e (turquoise) and the METAR-visibility estimated from the observers (green). The maximum visibility indicated by the RVRs is 2000 m, the observers estimate visibilities up to 10 km. z denotes the height above the radar antenna ($=\text{range} \cdot \sin(5^\circ)$). Similar images of the other 16 days can be seen at <http://metekgmbh.dyndns.org/jportfog>.

The data from one selected day with persistent fog is shown in Fig. 5. The height-time cross sections of the radar reflectivity Z together with the visibilities measured by the RVR instrument installed closest to the cloud radar, and the visibility estimated by the observers in the Tower for the half hourly METAR report.

The METAR visibility corresponds to an average over the altitude from 50 m to ground, the RVR measurements are made at 2 m AGL. This explains much of the differences between these two measurements. Particularly in case of deep fog layers, as can be seen in the radar data as in Fig. 5, the RVRs tend to indicate much higher visibility than then cloud radar (lowest height 16 m) or the human observer (at 25 m). The process responsible for this discrepancy is probably the near-surface fog dissipation due to fog collection by vegetation (here mainly blades of grass) in conjunction with reduced radiative fog production due to counter radiation by the deep fog layer.

The plots in Fig. 6 and 7 show scatter plots of the radar reflectivity from the range gate at 28 m AGL versus the RVR- or METAR-visibility respectively. Instead of plotting dots (one for each pair of data) the local density of dots is presented by color coding.

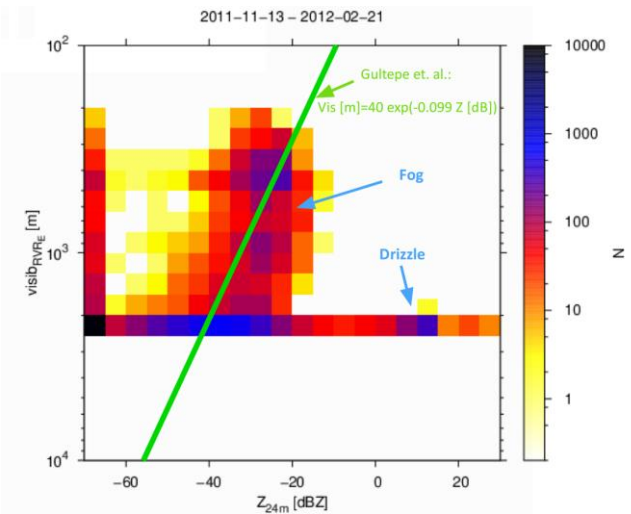


Fig 6: Scatter plot of the radar reflectivity of the range gate 10 (28 m AGL) versus the visibility length measured by the nearest RVR instrument. The data from the 17 days having fog events is comprised. The green line is a Z -Vis relation found by Gultepe et al. (see section 4.2)

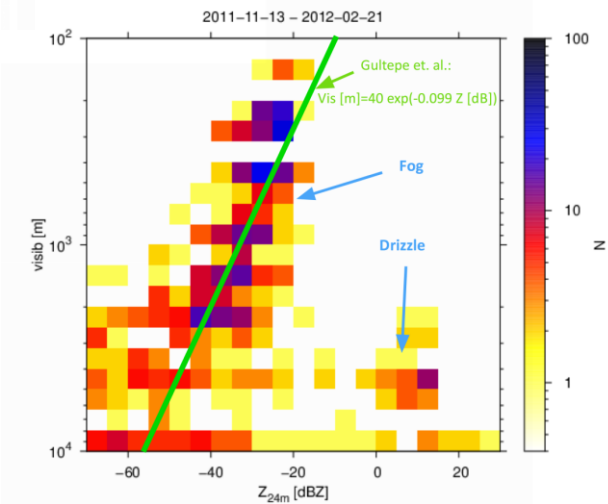


Fig 7: Same as Fig 6 but using the METAR visibilities estimated by the human weather observer in the tower..

Both scatter plots show a useful correlation in the dBZ range from -55 to -20 dBZ. Although most rain events where filtered some moderate rain or drizzle is probably still in the data causing the peak at about $+10$ dBZ and good visibility. The dBZ values of drizzle and rain seem to be well separated from the dBZ values of fog ranging from -60 to -20 dBZ.

Using the RVR visibilities provides better statistics than the METAR visibilities, as the latter are available only once per 30 minutes. On the other hand the METAR visibilities represent the altitude region where Z values from the radar are available, while the RVR visibilities

represent altitudes below the lowest radar level. Therefore the METAR visibilities were used for investigating the Z-Vis relation. The best correlation was achieved by using the Z values of the range gate at 28 m AGL. With this data a coarse Z-Vis relation has been determined by a linear fit:

$$Vis [m] \sim -137 Z [dBZ] - 2609 \quad (1)$$

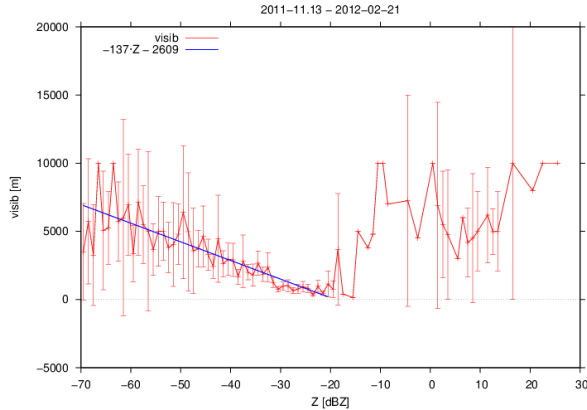


Fig. 8: average and variance of visibilities reported in the METAR data sorted by the Reflectivity measures at the corresponding times.

The plot shown in Fig. 8 shows the average and variance of visibilities reported in the METAR data sorted by the Reflectivity measures at the corresponding times. Some of the variance is caused by the fact that the Observer is about 2 km away from the radar. Nevertheless the variance in the critical region of short visibilities is rather small, which indicates that in the region from -45 to -20 dBZ the Z-Vis relation (1) may be used to calculate the visibility from the reflectivity with a useful accuracy.

4. Z-VIS RELATIONS FROM OTHER AUTHORS

4.1. Theoretically calculated Z-Vis relation

Boers et al. (2012) provide a theoretically calculated Z-Vis relation which depends on the parameter k describing the hygroscopicity of the aerosols. They also made a field campaign with a Ka band cloud radar tilted to a low elevation and they had in-situ visibility sensors installed on a mast. Unfortunately their results are not in good agreement with ours. The theoretically calculated Z-Vis relation gives much shorter visibilities. Maybe also the radar calibrations are different.

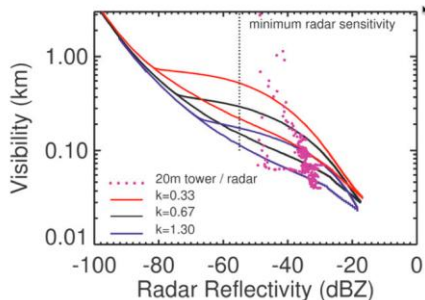


Fig. 9: Theoretically calculated Z-Vis relations from Boers et al. (2012). The dots show reflectivities measured by a Ka band cloud radar related to in situ visibility measurements made on a tower located close to the radar beam.

4.2. Z-Vis relation obtained from measured drop size distributions

If the drop size distribution is known the reflectivity Z and the visibility length MOR can be calculated:

$$Z = \int_0^{\infty} n(D)D^6 dD \quad (2)$$

where $n(D)$ density of droplets with a diameter D

$$MOR = -\frac{K}{\alpha} \quad (3a)$$

where $K = \ln 0,05$ is an empirical constant that relates the optical extinction α to a level that allow recognizing enough contrasts. The extinction can be calculated by

$$\alpha = \frac{\pi}{4} \int_0^{\infty} Q_{ext}(D, \lambda) n(D) D^2 dD \quad (3)$$

where λ is the wave length of visible light and Q_{ext} is the normalized extinction cross section. It is generally a complicated function of D and λ but in case of the droplet sizes contributing most to extinction in fog it can be approximated by the constant value 2.

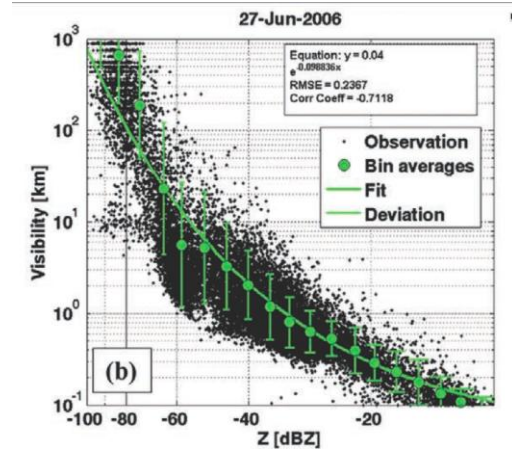


Fig 10: Z-Vis scatter plot. Z and Vis are calculated from drop size distributions measured during a 5 hour fog event with an in situ FMD device (SSP-DTM Inc.).

Using this approximation α is proportional to the second moment and Z to the 6th moments of the drop size distribution. If the distribution is shifted to larger droplets Z increases much more than Vis .

Gultepe et al. (2008) have obtained a Z-Vis relation by measuring drop size distributions during a fog event and calculating the visibility length Vis and the radar

reflectivity factor Z from the measured drop size distributions by (2) and (3). Their scatter plot from a 5 hour fog event is shown in Fig 10.

They fitted the following Z-Vis relation into the scatter plot:

$$Vis [m] = 40 e^{-0.099 Z [dBZ]}$$

This Z-Vis relation is plotted into the scatter plots shown in Fig. 6 and 7. Although the Z-Vis relation is gained by a very different approach it seems to agree well to our measurements in the range between -50 and -25 dBZ. As visibility is getting shorter the radar measured reflectivity seems to reach a saturation value at -20 dBZ. This may be caused by scattering at coherent droplet clusters (see Argyroulli et al. (2012)).

5. Method for deducing the visibility from Ceilometer and Radar data

The disadvantage of using the visibility data shown in Fig. 6 and 7 for investigating the Z-Vis relation is that they represent the visibility at other location than the radar beam. A ceilometer that was located below the radar beam can provide data that is nearly coincident with the radar beam at least at one range gate (see Fig. 11). For this reason a method has been developed to determine the meteorological optical rang (MOR) from the radar and the ceilometer data. Due to the extinction of optical waves this method is of course restricted to ranges in the order of MOR, which is in case of low visibility only a thin layer at the bottom of clouds or fog.

Retrieving the extinction coefficient only with the data of the ceilometer by the Klett algorithm (see Klett (1981)) does not work in case of fog. In contrast to the Klett-method the method described here does not require the reflectivity in a reference range.

5.1. Theoretical description of the method

The method makes use of the assumption that within a few range gates the changes of the reflectivity with height are the same for the radar and for the lidar. If this assumption is fulfilled the lidar signal decays faster than the radar signal because the extinction of the radar signal in fog is negligible whereas the extinction of the lidar signal is related by equation (3a) to the MOL or visibility Vis .

The radar reflectivity can be written as

$$Z(r_i) = \Gamma_R \beta_R(r_i)$$

It depends only on the range of the i -th range gate r_i and the volume scattering cross section β_R in this range gate. The constant Γ_R contains the radar constant and other factors that don't depend on the range.

The calibrated signal intensity received by the ceilometer can be written as

$$m(z_i) = \Gamma_L O(z_i) \beta_L(z_i) \exp \left\{ \underbrace{-2 \int_0^{z_i} \alpha(\zeta) d\zeta}_{\tau(z_i)} \right\}$$

Here m is the lidar backscatter coefficient as provided by the lidar. It is biased with respect to the true lidar backscatter coefficient $\beta_L(z_i)$ due to the calibration error Γ_L , the overlap function $O(z_i) < 1$ describing the overlap between the transmitting and the receiving beams and the path attenuation (described by the extinction coefficient $\alpha(\zeta)$ on the way between lidar and scattering volume or the two-way transmission $\tau(z_i)$).

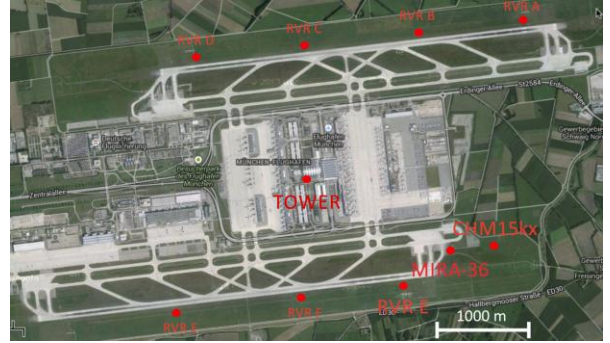


Fig. 11: Location of the cloud radar and the ceilometer on the Munich airport. The distance between the radar and the ceilometer is 386 m. During the gliding path measurements the radar beam is directed towards the ceilometer so that at a height of 35 m above the ceilometer both beams overlap.

To eliminate the unknown factors, another approach using the radar and the ceilometer data has been chosen. For this method we calculate the ratios of the lidar and the radar signal intensities at two range gates:

$$Q(z_i) = \frac{\Gamma_L O(z_i) \beta_L(z_i) \tau(z_i)}{\Gamma_R \beta_R(z_i)}$$

and

$$Q(z_{i+1}) = \frac{\Gamma_L O(z_{i+1}) \beta_L(z_{i+1}) \tau(z_{i+1})}{\Gamma_R \beta_R(z_{i+1})}$$

Then we calculate the ratio of the ratios calculated for two range gates above

$$A(z_{i+1}, z_i) = \frac{O(z_{i+1}) \beta_L(z_{i+1}) \tau(z_{i+1}) \beta_R(z_i)}{O(z_i) \beta_L(z_i) \tau(z_i) \beta_R(z_{i+1})} \quad (5)$$

The constant factors Γ_L and Γ_R cancelled out in equation (5). This means that $D(z_{i+1}, z_i)$ does not depend on errors of the instrument calibrations. (I.e. it does not depend on the calibration at all.)

Now we introduce the key-assumption that

$$\frac{\beta_R(z_i)}{\beta_L(z_i)} = \frac{\beta_R(z_{i+1})}{\beta_L(z_{i+1})} \quad (6)$$

We emphasize that we do not postulate a globally constant ratio β_R/β_L . This would be in fact not justified because the dependence of β_R and β_L on variations of the drop size distribution is very different. It is only assumed that the drop size distributions in adjacent range gates z_i and z_{i+1} are similar, which means that they may differ only by a constant (size-independent) factor but agree in shape otherwise. Since β_R and β_L are linear dependent on the spectral number density, equation (6) holds in this case.

We must keep in mind that even this restricted assumption is not generally valid: If one or both range gates are outside of a cloud/fog the corresponding β -values and consequently the ratios in equation (6) may be noisy. Such case can be recognized easily by its low β -values. Another less obvious example, where equation 6 does not hold, is a drizzling cloud. Here the lower cloud boundary marks a transition between very different drop size distributions. The cloud drop fraction – existing within the cloud – is missing in the drizzle curtain below the cloud. Such case can nevertheless be sorted out using the Doppler shift of radar echoes from (falling) precipitation. Here we assume for simplicity that both range gates are inside of a non-precipitating cloud/fog-layer.

With validity of equation (6) all β -factors cancel out in equation (5), and it reduces to

$$A(z_{i+1}, z_i) = \frac{O(z_{i+1})\tau(z_{i+1})}{O(z_i)\tau(z_i)}$$

The overlap function is not known, but we may at least assume that the ratio $O_{i,i+1} \equiv O(z_{i+1})/O(z_i)$ is constant with time, and we obtain

$$A(z_{i+1}, z_i) = O_{i,i+1} \exp\left\{-2 \int_{z_i}^{z_{i+1}} \alpha(\zeta) d\zeta\right\}$$

or

$$A(z_{i+1}, z_i) = O_{i,i+1} \exp\{-2\alpha(z_{i+1}, z_i)\Delta z\} \quad (9)$$

with $\alpha(z_{i+1}, z_i)$ extinction between range gate i and $i + 1$. Equation (9) can be resolved for $\alpha(z_{i+1}, z_i)$:

$$\alpha(z_{i+1}, z_i) = \frac{1}{2\Delta z} (\ln O_{i,i+1} - \ln A(z_{i+1}, z_i))$$

The unknown term $\ln O_{i,i+1}$ on the right side can be estimated from larger set of measurements of $\ln A(z_{i+1}, z_i)$ and using the fact that $\alpha(z_{i+1}, z_i)$ cannot fall below zero, as this would correspond to unrealistic negative extinction. $O_{i,i+1}$ is then adjusted such that the minimum value of $\alpha(z_{i+1}, z_i)$ is zero.

5.2. Results from using the radar/lidar method for calculating the visibility

The height resolution of the ceilometer is 15 m. Taking the elevation angle of the radar into account the height resolution of the radar was 2.5 m. The radar data was

gridded to the height scale of the ceilometer. For the calculation of the extinction we tried using the following pairs of heights: 30 m:45 m, 30 m:60 m, and 30 m:90 m. The second pair with a delta of 30 m worked best.

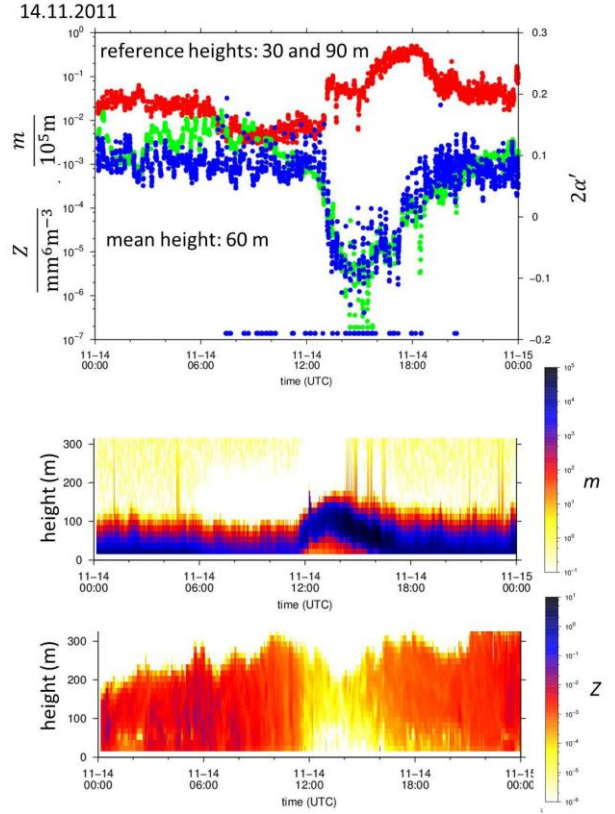


Fig 12: Example of fog episode. Upper panel: Time series of attenuated lidar backscatter coefficient m (red), radar reflectivity factor Z (green) and biased extinction coefficient α (blue) using the reference heights 30 and 90 m. Middle panel: Time height cross section of β . Lower panel: Time height cross section of Z .

The radar/lidar visibilities resulting from this method depend much on the correction factor $O_{i,i+1}$ for correcting the overlap function. To show this we made scatter plots of the radar/lidar visibilities calculated with different values of $O_{i,i+1}$ versus the METAR visibilities (see Fig. 13).

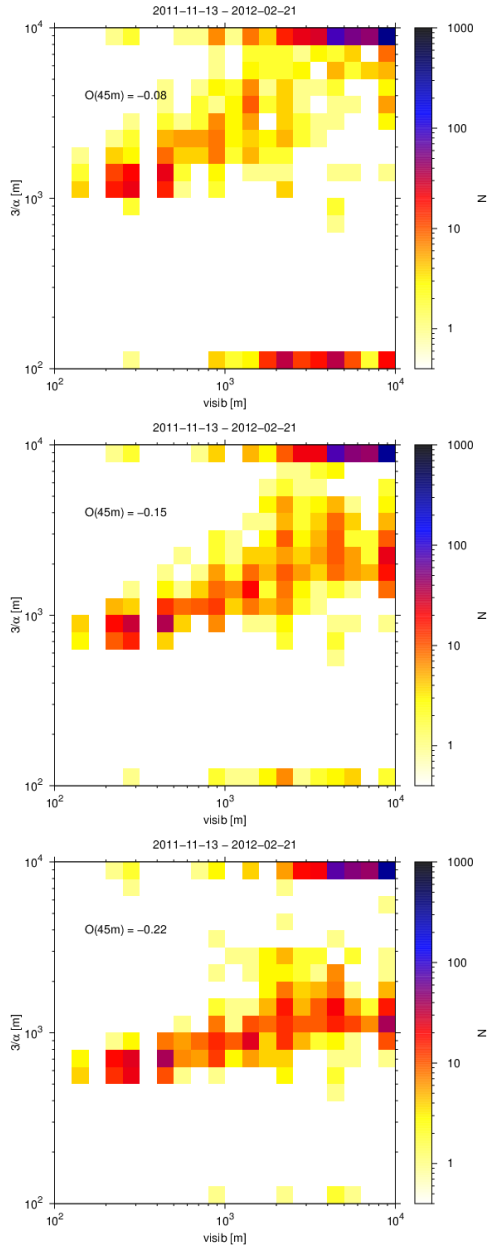


Fig. 13: Scatter plots of the METAR visibilities versus the visibility calculated by the radar/lidar method (3α) assuming three different values of $O_{i,i+1}$.

If $O_{i,i+1}$ is chosen smaller then the visibilities resulting from of the radar/lidar method are larger and it happens more frequently that the extinctions become negative (collapsed to 10^2 in the plots). $O_{i,i+1} = -0.15$ seems to be a good compromise.

The plots also show in situations with short visibilities the radar/lidar method overestimates the visibility length. This is independent of the choice of $O_{i,i+1}$. This is probably caused by multi path scattering in case of strong fog which produces signals that return with a delay that fakes a range which is beyond the visibility length. It seems that the ceilometer does not show a big

difference between fog with moderate and short visibilities. Without taking multi scattering into account the radar/lidar visibilities cannot be used for deriving a more accurate Z-Vis relation.

6. Monitoring of advected fog banks by RHI scans

At the end of the experiment the radar was configured for making 20 RHI scans per hour between 3 and 177° elevation. The intention was to observe the advection of cloud banks across the airport for investigating the potential of short range prediction of the local fog development. These preliminary attempts were not conclusive because the spatial extension of the few observed fog events was beyond the maximum range of the radar. A noteworthy side result of these scans is the analysis of Doppler velocities showing the capability to determine horizontal wind velocity profiles (component in the RHI-plane) and even the fall velocity profile of the fog droplets (see Fig. 14). It seems that the influence of turbulent variations of the vertical wind is effectively eliminated due to averaging over large horizontal areas. Also on fog the vertical wind turbulence is much smaller than in clouds. It can be seen that the falling velocity of the droplets increases with distance from the fog top. Case studies show that in case of thick cloud layers the visibility calculated from Z by using the Z-Vis relation often underestimate the visibility. This may be caused by drizzle droplets which give a large contribution to Z but not much contribution to the Visibility. The beginning of drizzle may be detected by the vertical velocity estimates from RHI scans and this may be used to improve visibility estimate from the radar data.

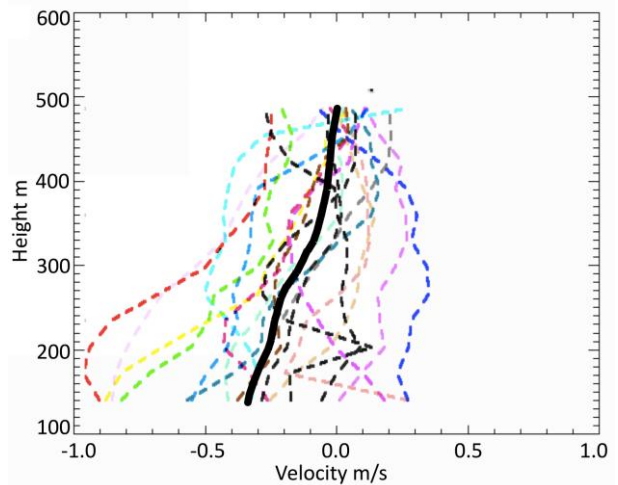


Fig.14: Falling velocity profiles deduced the radial velocities of 20 RHI scans assuming horizontal homogeneity. Each dashed line is calculated from the data of one RHI scan. The thick line is the average of the 20 scans which were made in one hour.

Argyrouli, A., Neil Budko¹, Herman Russchenberg², and Christine Unal, 2012: The Effect of Droplet Clustering on the Statistics of Radar Backscatter from

Water Clouds. 9th International Symposium on Tropospheric Profiling (ISTP).

Boers, R., H. Klein Baltink, H. J. Hemink, F. C. Bosveld, M. Moerman, 2013: Ground-Based Observations and Modeling of the Visibility and Radar Reflectivity in a Radiation Fog Layer. *J. Atmos. Oceanic Technol.*, 30, 288–300.

Gultepe, I. G. Pearson, J. A. Milbrandt, B. Hansen, S. Platnick, P. Taylor, M. Gordon, J. P. Oakley, and S. G. Cober, 2009: The Fog Remote Sensing and Modeling Field Project. *Bull. Amer. Meteor. Soc.*, 90, 341–359.

Klett, J. D.: Stable Analytical Inversion Solution for Processing Lidar Returns. *Appl. Opt.* **20** (1981) 211–220

Acknowledgment

The iPort project was funded by the German government, and the scanning cloud radar used during the field campaign was provided by Forschungszentrum Juelich.

gefördert durch
das BMWi



Bundesministerium
für Wirtschaft
und Technologie